Available online at www.sciencedirect.com

SCIENCE DIRECT

ELSEVIER

Earth and Planetary Science Letters 244 (2006) 83–96

EPSL

www.elsevier.com/locate/epsl

The airborne lava–seawater interaction plume at Kīlauea Volcano, Hawai‘i

M. Edmonds [a,*], T.M. Gerlach [b]

[a] *United States Geological Survey, Hawaiian Volcano Observatory, 51 Crater Rim Drive, Hawai‘i National Park, Hawai‘i 96718, United States*
[b] *United States Geological Survey, Cascades Volcano Observatory, 1300 Cardinal Court #100, Vancouver, Washington 98683-9589, United States*

Received 24 May 2005; received in revised form 17 January 2006; accepted 3 February 2006
Available online 13 March 2006
Editor: V. Courtillot

Abstract

Lava flows into the sea at Kīlauea Volcano, Hawai‘i, and generates an airborne gas and aerosol plume. Water (H_2O), hydrogen chloride (HCl), carbon dioxide (CO_2), nitrogen dioxide (NO_2) and sulphur dioxide (SO_2) gases were quantified in the plume in 2004–2005, using Open Path Fourier Transform infra-red Spectroscopy. The molar abundances of these species and thermodynamic modelling are used to discuss their generation. The range in molar HCl/H_2O confirms that HCl is generated when seawater is boiled dry and magnesium salts are hydrolysed (as proposed by [T.M. Gerlach, J.L. Krumhansl, R.O. Fournier, J. Kjargaard, Acid rain from the heating and evaporation of seawater by molten lava: a new volcanic hazard, EOS (Trans. Am. Geophys. Un.) 70 (1989) 1421–1422]), in contrast to models of Na-metasomatism. Airborne droplets of boiled seawater brine form nucleii for subsequent H_2O and HCl condensation, which acidifies the droplets and liberates CO_2 gas from bicarbonate and carbonate. NO_2 is derived from the thermal decomposition of nitrates in coastal seawater, which takes place as the lava heats droplets of boiled seawater brine to 350–400 °C. SO_2 is derived from the degassing of subaerial lava flows on the coastal plain. The calculated mass flux of HCl from a moderate-sized ocean entry significantly increases the total HCl emission at Kīlauea (including magmatic sources) and is comparable to industrial HCl emitters in the United States. For larger lava ocean entries, the flux of HCl will cause intense local environmental hazards, such as high localised HCl concentrations and acid rain.

Keywords: ocean entry; lava flows; hydrogen chloride; magnesium chloride; plume; aerosol; Kīlauea

1. Introduction

When magma interacts with water, the results can be explosive and violent, at other times gentle and benign. At Kīlauea Volcano, Hawai‘i, basaltic lava usually flows into the sea in a passive manner, with the interaction confined to the boiling of seawater. Occasionally, larger lava ocean entries are associated with explosive activity as seawater invades confined lava tubes [2]. This paper focuses on the chemical interactions which take place as seawater boils and evaporates extensively at the low pressures of the ocean surface and creates a halogen-rich, acidic, airborne plume [1,3,4]. Previous work has identified the main component of the condensed plume as hydrogen chloride [1,5,6].

This study presents the gas composition of the airborne lava–seawater interaction plume derived from a novel application of Open Path Fourier Transform

* Corresponding author. Tel.: +1 808 9678845; fax: +1 808 9678890.
E-mail address: medmonds@usgs.gov (M. Edmonds).

0012-821X/$ - see front matter © 2006 Elsevier B.V. All rights reserved.
doi:10.1016/j.epsl.2006.02.005

infra-red Spectroscopy (OP FTS). The OP FTS spectra were collected remotely (50–120 m), using the incandescent lava flowing into the sea as a source of infra-red radiation. The cold gases in the plume absorbed characteristic wavelengths of the radiation, which was then received by the spectrometer. The measured HCl/H_2O molar ratios are used to distinguish between two models for HCl generation in the airborne lava–seawater interaction plume: the hydrolysis of magnesium chloride on boiling seawater to dryness [1] and reactions involving steam and sodium chloride in seawater [4]. The origins of the other constituents of the plume are interpreted with reference to the chemical and thermal processes taking place as lava interacts with seawater. Estimates of the mass flux of HCl gas from the lava entry site are compared to that from Pu'u 'Ō'ō and from industrial sources in the United States. These results are extrapolated to large eruptions of Mauna Loa and Kīlauea volcanoes and their implications discussed.

2. Methodology

On 21 and 28 July 2004, lava was emerging from tubes on the lava delta and flowing into the sea as several continuous streams of lava, each a few tens of centimetres to a few metres wide (Fig. 1a,b). During lava entry into the sea, a dense, white plume arose and drifted downwind (Fig. 1c). On 21 July onshore breezes carried the plume to the west–northwest and, on 28 July, westwards. The large volcanic plume from Pu'u 'Ō'ō drifted southwest on both days and consequently did not mix with the lava–seawater interaction plume. OP FTS measurements were made 80 m northeast of the lava ocean entry on 21 and 28 July 2004 (Fig. 1d) and on 6 and 20 February 2005, 150 m west of the entry. On 6

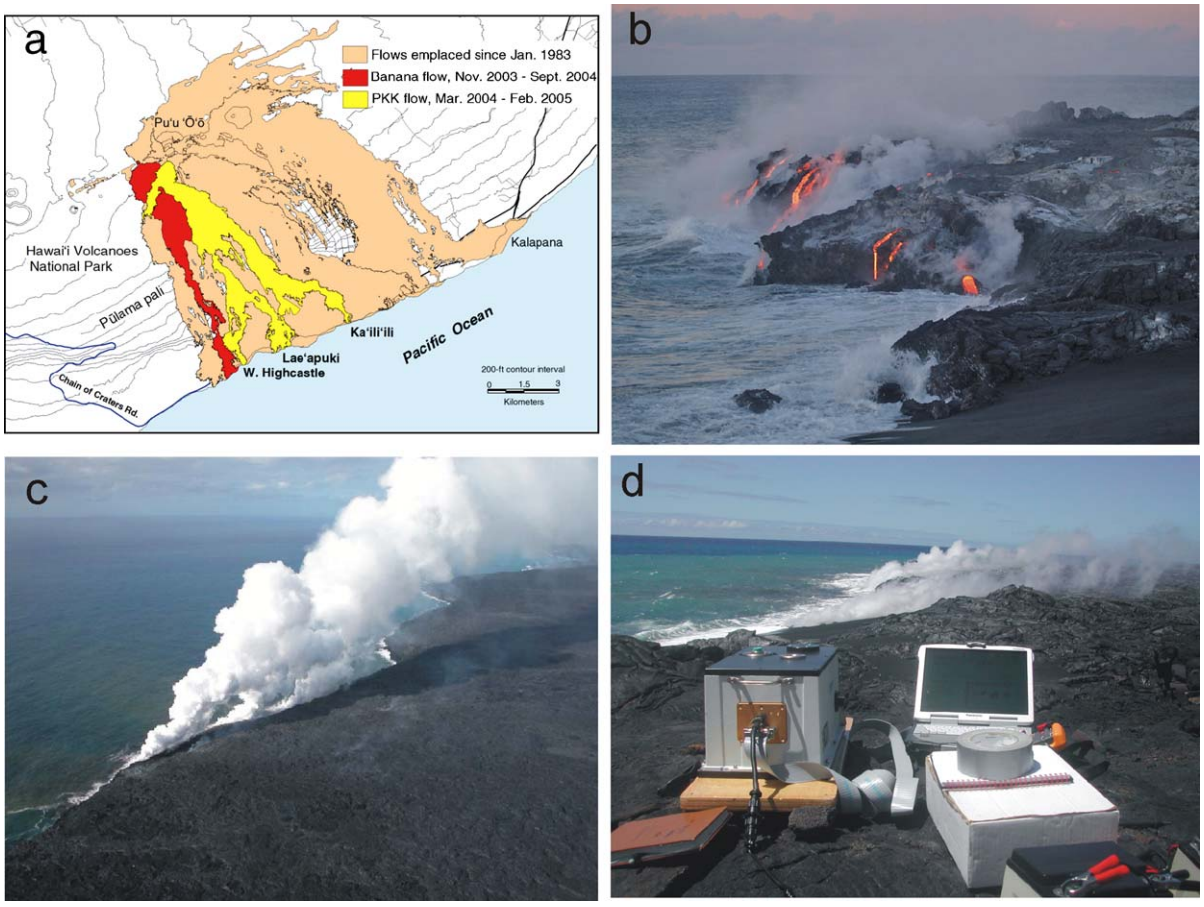

Fig. 1. (a) Map of the coastal plain and lava ocean entry, compiled by C. Heliker; (b) the lava flow ocean entry on 20 July 2004, photograph by D. Swanson; (c) dense, opaque plume rising from the lava flow ocean entry 4 March 2005, photograph by T. Orr; (d) photograph to show the instrument configuration for measurements, using the lava as an IR source and the dense lava–seawater interaction plume passing between the source and the spectrometer.

February the lava entry into the sea was vigorous; on 20 February 2005, the flux of lava reaching the sea appeared greatly diminished. Estimates of the mean lava flux into the sea are derived from calculations of the volume of lava necessary to account for the SO_2 released from Pu'u 'Ō'ō [7].

A MIDAC spectrometer with a stirling-cooled InSb detector, which has a field of view of 0.5 m at 80 m, was used for the measurements. The aperture of the spectrometer was aligned with a consistently glowing lava flow, which served as the source of IR radiation, just above the point at which it flowed into the sea. The plume rose from where the lava was entering the sea, immediately in front of the IR source (Fig. 1d), allowing measurements of a very young plume (a few seconds). Intermittent stagnation of the flow into the sea was accompanied by a decrease in the vigour of the gas plume, but the IR source was still sufficiently hot to maintain a consistent signal-to-noise ratio. For each measurement, eight spectra were averaged, yielding a sampling rate of 4 single beam spectra per minute. The spectra record the wavelength and intensity of IR radiation between 1800 and 4000 cm^{-1}. For analysis, Autoquant4 (MIDAC Corp.) was used, based on the principles of Beer's Law:

$$A_i = \sum_{j=1}^{M} a_{ij} \mathrm{LC}_j, i = 1, 2 \ldots N \quad (1)$$

where M is the number of compounds absorbing in the spectral region analyzed, A_i is the observed sample absorbance at frequency i, C_j is the (unknown) concentration of component j, L is the absorption pathlength used in recording the spectrum, and a_{ij} is the absorptivity of compound j at infra-red frequency i. The absorbance spectrum, A_j, for each species is obtained by normalizing the measured spectrum which contains absorptions S_j, by a background spectrum B, which is free of, or contains less of, the species:

$$A_j = -\log\left(S_j/B\right). \quad (2)$$

In practice, every spectrum contained HCl gas and, hence, the background also contained a small amount: the pathlength-concentration values are minimum values. Calibration spectra for pure components at known concentrations are used to calculate the absorptivities a_{ij}. Species analysed for were water (H_2O), carbon dioxide (CO_2), hydrogen chloride (HCl), nitrogen dioxide (NO_2), sulphur dioxide (SO_2), methane (CH_4) and carbon monoxide (CO). Table 1 shows the regions used for fitting, detection limits, and errors on the measurements.

Table 1
Wavenumber regions used for the fitting of laboratory spectra to measured spectra

Species	Wavenumber window (cm^{-1})	Detection limit (ppm mv)	Error (%)
H_2O	2143.86–2154.44	4000	8.4
CO_2	2075.00–2079.59	2000	12
HCl	2705.16–2834.02	3	2.8
NO_2	2913.25–2922.52	10	25
SO_2	2470.28–2532.63	5	9.8

Detection limits were obtained by comparing the average background amplitude in the fitting region to the absorption feature of the species concerned. Detection limits are high for species present in the background air, such as CO_2 and H_2O. HCl is the only species with low detection limits and errors, owing to its strong and fast absorption feature in the region of no interference with other species and its low abundance in the background air. Average errors were calculated from the mean of the percentage error on each spectral retrieval. Errors on NO_2 are high owing to some interference with the H_2O absorbance feature, although the fast nature of the NO_2 absorbance spectrum ensures a reasonably low detection limit. SO_2 is a weak absorption feature, although the spectral noise in this region is very low and therefore SO_2 can be detected at 5 ppm m.

3. Results

The lava–seawater plume contained H_2O, CO_2, HCl, NO_2 and SO_2 above limits of detection (CO and CH_4 were below detection). Fig. 2 shows pathlength-concentrations of these five species plotted against time for 28 July 2004, 6 and 20 February 2005, and Table 2 shows the calculated mean and maximum pathlength-concentrations and estimated mean and maximum plume concentrations for each species for the four days of measurements. Fig. 2 and Table 2 show that CO_2, NO_2, and SO_2 were below detection on 21 July 2004 and NO_2 was below detection on 28 July 2004. The pathlength-concentrations increased and decreased over time (Fig. 2). This suggests that either their generation was variable in rate or the abundance and/or concentrations of the species were affected by changing wind patterns. Fig. 3 shows H_2O, CO_2, NO_2, and SO_2 plotted against HCl. The lack of a good correlation between species was due to both rapid changes in plume chemistry as, for example, water condensed from steam and dissolved water-soluble components and to multiple and variable sources for the plotted species (discussed later). The mean molar ratios between each species and HCl are similar on all of the days of measurement,

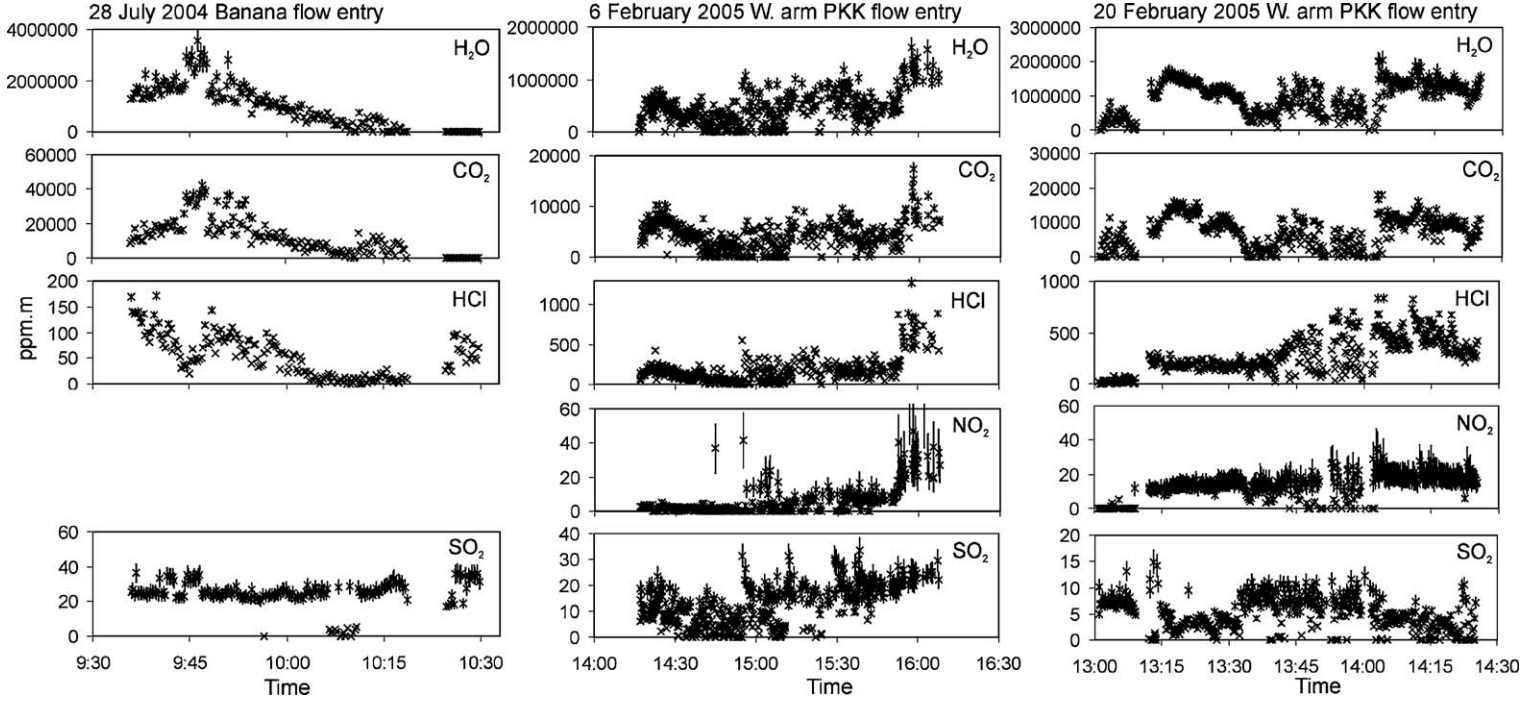

Fig. 2. H_2O, CO_2, HCl, NO_2 and SO_2 pathlength-concentrations (in units of ppm m by volume) over time for left: 28 July 2004 (NO_2 below detection); middle: 6 February 2005 and right: 20 February 2005.

Table 2
Composition of the airborne lava–seawater interaction plume measured by OP FTS on 21 and 28 July 2004 and 6 and 20 February 2005

Date		$(CL)_{mean}$ (ppm m)	$(CL)_{max}$ (ppm m)	$C_{mean(L)}$ (ppm)	Plume concentration range	
					$C_{mean(plume)}$ (ppm)	$C_{max(plume)}$ (ppm)
21-July-04 $n=100$	H_2O	1.23×10^5	2.94×10^5	1.54×10^3	4.1×10^3	9.8×10^3
	CO_2	bd	bd	bd	bd	bd
	HCl	22.4	65.4	0.280	750 ppb	2.2
	NO_2	bd	bd	bd	bd	bd
	SO_2	bd	bd	bd	bd	bd
28-Jul-04 $n=220$	H_2O	7.97×10^5	3.55×10^6	9.96×10^3	2.7×10^4	1.2×10^5
	CO_2	9.75×10^3	4.22×10^4	122	330	1400
	HCl	46.0	172	0.575	1.5	5.7
	NO_2	bd	bd	bd	bd	bd
	SO_2	24	38	0.30	800 ppb	1
6-Feb-05 $n=800$	H_2O	4.29×10^5	1.60×10^6	2.86×10^3	1.4×10^4	5.4×10^4
	CO_2	3.99×10^3	1.74×10^4	26.6	130	580
	HCl	161	1270	1.07	5.4	42
	NO_2	6.2	65	0.041	200 ppb	2
	SO_2	12	34	0.082	400 ppb	1
20-Feb-05 $n=520$	H_2O	9.46×10^5	2.05×10^6	630×10^3	3.2×10^4	6.8×10^4
	CO_2	7.08×10^3	1.79×10^4	47.2	240	600
	HCl	269	833	1.80	9.0	28
	NO_2	14	35	0.092	500 ppb	1
	SO_2	5.0	15	0.034	200 ppb	500 ppb

Columns three and four are pathlength-concentration products, which are calculated directly from the absorbance spectra. $(CL)_{mean}$ is the mean pathlength-concentration, calculated from n spectra (value of n given in column one) and $(CL)_{max}$ is the maximum pathlength concentration. Columns five to seven are concentrations, derived by dividing the pathlength-concentration product by the pathlength. Column five, $C_{mean(L)}$, is derived from dividing column one by a total pathlength of 80 m for the July 2004 measurements and 150 m for the February 2005 measurements and has units of ppm. Only a fraction of the total pathlength is plume, so columns six and seven together provide a range of expected concentrations of each species in the plume using an estimate of plume width (30±5 m for all measurements, estimated from photographs and detailed maps). $C_{mean(plume)}$ uses column three divided by the estimated plume width to provide a mean value for plume concentrations and column seven, $C_{max(plume)}$, uses column four, $(CL)_{max}$, to provide an estimate of possible maximum plume concentrations. The number of significant figures reported are according to species and/or plume width estimate; bd: below detection.

however, with the exception of HCl/SO_2, which varied considerably (Table 3).

Average pathlength-concentrations for water (steam) ranged between 1.23×10^5 and 9.46×10^5 ppm m; and estimated mean plume concentrations reached $\sim3.2\times10^4$ ppm on 20 February 2005 (Table 2). The steam was derived from the boiling of seawater. Molar HCl/H_2O in the plume ranged from 5.8×10^{-5} on 28 July 2004 to 3.8×10^{-4} on 6 February 2005 (Table 3). CO_2 was present in the plume above background on 28 July 2004 and 6 and 20 February 2005 at average pathlength-concentrations of 3.99×10^3 (on 6 February 2005) to 9.75×10^3 ppm m (on 28 July 2004). Average plume concentrations (above background) of CO_2 ranged from 130 ppm on 6 February 2005 up to 330 ppm on 28 July 2004 and probably reached 1400 ppm in the proximal plume on 28 July 2004 (Table 2). CO_2 was below detection on 21 July 2004.

Mean HCl pathlength-concentrations of 22.4 ppm m were measured on 21 July 2004 and 269 ppm m on 20 February 2005. Estimates of average plume concentrations yield 750 ppb and 9.0 ppm on these days, respectively. On 6 February 2005 plume concentrations reached 42 ppm near to the lava–seawater interaction plume source. In the 1990 measurements [3], concentrations of HCl averaged 6.4 ppm over a sampling time of 5 min in the plume and 9–11 m from the point of origin, with a maximum of 12 ppm. At similar distances from the source, 10–15 ppm HCl was reported in Kalapana in 1990 [8] (Fig. 1a). A rapid decrease in HCl concentration with distance has been documented previously [3], probably due to dilution and/or the rapid removal of HCl from the plume by condensation into water droplets.

NO_2 was below detection in July 2004, but at average pathlength-concentrations of 6.2 ppm m on 6 February and 14 ppm m on 20 February. Estimated mean plume concentrations were 200 and 500 ppb, respectively and maximum concentrations were 2 ppm on 6 February (Table 2). In the study conducted by [3], indicator tubes failed to detect NO_2 gas, probably due to dilution of the plume downwind.

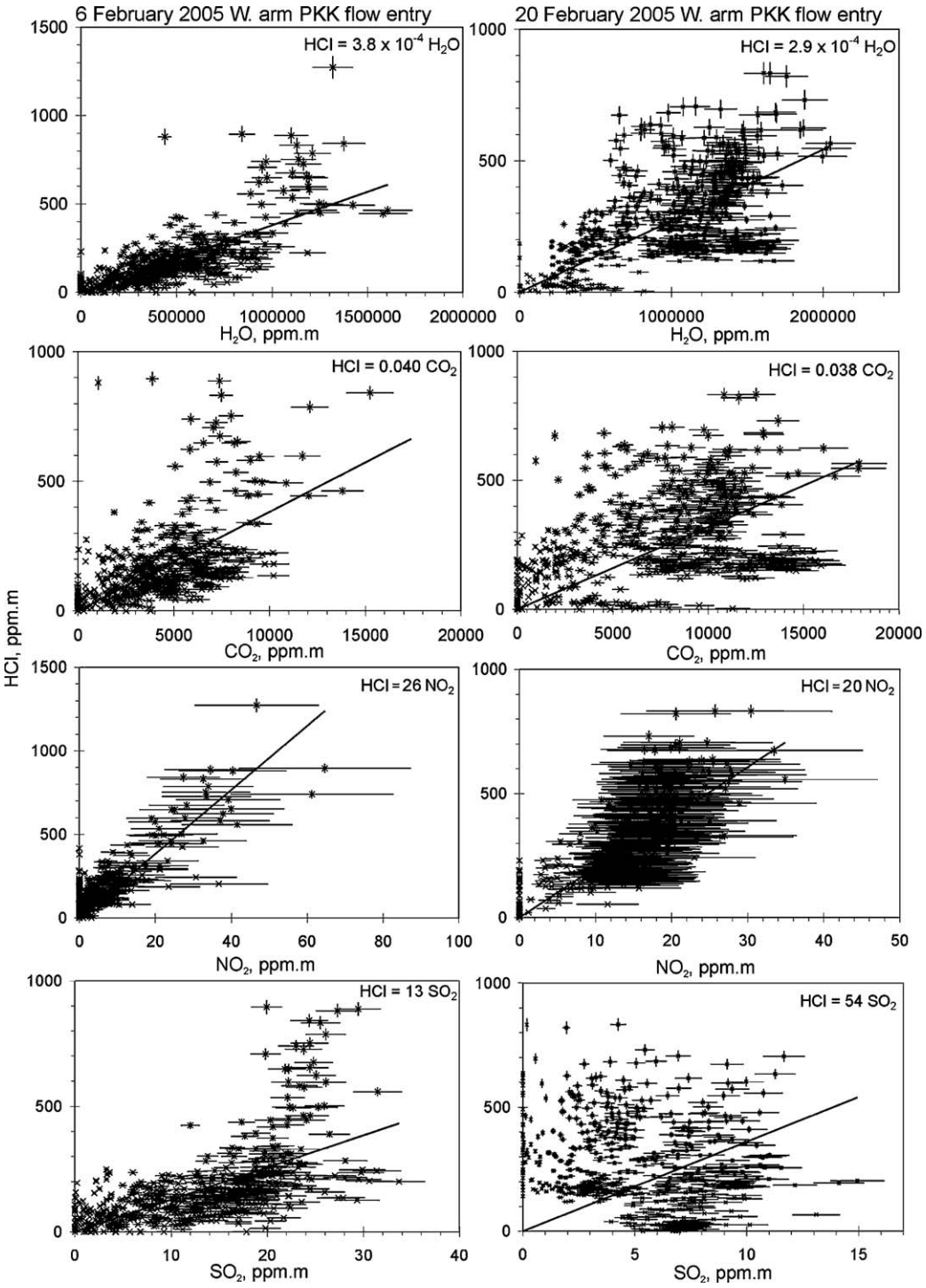

Fig. 3. Covariation of HCl with H_2O, CO_2, NO_2 and SO_2 for left: 6 February 2005 and right: 20 February 2005. Units are pathlength-concentrations in ppm m by volume.

SO_2 was below detection on 21 July 2004, but had a mean pathlength-concentration of 24 ppm m on 28 July 2004, 12 ppm m on 6 February 2005 and 5 ppm m on 20 February 2005 (Table 2). Estimated concentrations over the entire pathlength are 300 ppb on 28 July 2004, 82 ppb on 6 February and 34 ppb on 20 February 2005

Table 3
Mean molar ratios for the OP FTS measurements taken at the lava ocean entry

Date	HCl/H_2O	HCl/CO_2	HCl/NO_2	HCl/SO_2
21-Jul-04	1.8×10^{-4}	1.0×10^{-2}	–	–
28-Jul-04	5.8×10^{-5}	4.7×10^{-3}	–	1.9
6-Feb-05	3.8×10^{-4}	4.0×10^{-2}	26	13
20-Feb-05	2.9×10^{-4}	3.8×10^{-2}	20	54

(Table 2). HCl/SO_2 molar ratios are variable in the plume on these three days, ranging from 1.9 on 28 July 2004 to 54 on 20 February 2005 (Table 3).

4. Discussion

4.1. Origin of HCl in the lava–seawater interaction plume

Fig. 4 shows absorbance spectra collected at the lava–seawater plume, a coastal plain lava flow and from a crater vent at Pu'u 'Ō'ō. Reference absorbance spectra show the idealised absorptions for SO_2, HCl and H_2O. The Pu'u 'Ō'ō spectrum clearly records the presence of all three species, but the lava–seawater plume spectrum contains HCl and H_2O only and the coastal plain gas contains H_2O only. The lack of HCl released from lava on the coastal plain (Fig. 4) indicates the origin of the HCl gas is seawater and not magmatic degassing from the subaerial lava flows, consistent with the conclusions of other workers [1,4]. The "acrid smell of HCl acid" was reported upon seawater splashing up onto the hot lava flows in 1969–1972 [6]. They ascribed the formation of HCl to the heat-induced dissociation of sodium chloride (NaCl) when lava flowed over the salt crust left on the surface of the shoreline. Two contrasting models of HCl gas generation during lava–seawater interaction are considered. HCl aerosol production was explained previously by several possible reactions involving NaCl from seawater and steam at high temperatures, to produce gaseous HCl, followed by dissolution of HCl into condensed water droplets [4]. The simplest such reactions involved NaCl and steam as reactants and either sodium hydroxide (NaOH) or a sodium silicate ($Na_2Si_2O_5$) and HCl gas as products. These schemes were rejected on the basis they would raise the pH of local seawater around the ocean entry; the opposite is observed [4]. Instead, they favoured reactions involving NaCl, H_2O and an aluminosilicate phase derived from the basalt, such as:

$$6SiO_{2(s,l)} + Al_2O_{3(s,l)} + 2NaCl_{(s,l)} + H_2O_{(g,l)} \rightarrow 2NaAlSi_3O_8 + 2HCl_{(g)}. \quad (3)$$

They also considered the incomplete hydrolysis of silicate, followed by the exchange of hydrogen ions with cations from seawater, which would yield HCl gas and an Al-silicate phase [4]. Significant involvement of magnesium chloride ($MgCl_2$) was rejected as a main reactant in the generation of HCl gas [4] owing to its lower abundance in seawater (seawater contains 5.4 times more NaCl than $MgCl_2$ by mass; Table 4). Alternatively, it has been proposed that the heat added to seawater from the

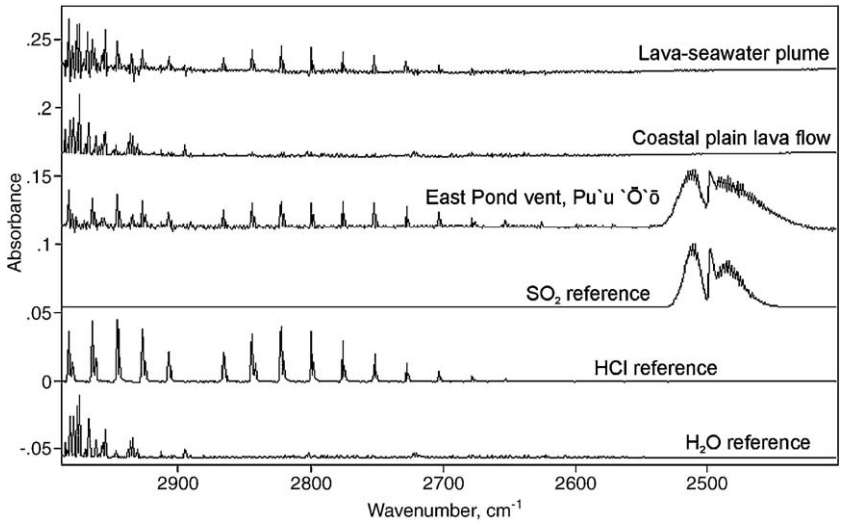

Fig. 4. Absorbance spectra for (from top to bottom) the lava–seawater plume 28 July 2004, gas issuing from a crack in the ceiling of a lava tube 3 km from the coast 6 August 2004, the volcanic plume from East Pond vent in Pu'u 'Ō'ō crater in March 2004, reference spectra for SO_2, HCl and H_2O. The absorbance axis numbering is for the HCl reference spectrum.

Table 4
Mean composition of North Pacific seawater, showing species for each element present at concentrations >100 ng/kg [9]

Element	Species	Mean conc., ng/kg
Sulphur	SO_4^{2-}	898×10^6
Nitrogen	Dissolved N_2	8.3×10^6
	NO_3^-	0.42×10^6
Strontium	Sr^{2+}	7.8×10^6
Bromine	Br^-	67×10^6
Phosphorus	Reactive PO_4	62×10^3
Iodine	I(V)	58×10^3
Calcium	Ca^{2+}	412×10^6
Boron	Borate	4.5×10^6
Potassium	K^+	399×10^6
Uranium		3.2×10^3
Carbon	Inorganic CO_2	27.0×10^6
Oxygen	Dissolved O_2	2.8×10^6
Silicon	Reactive SiO_2	2.8×10^6
Vanadium		2.0×10^3
Chlorine	Cl^-	19.35×10^9
Lithium	Li^+	180×10^3
Barium	Ba^{2+}	15×10^3
Sodium	Na^+	10.78×10^9
Molybdenum		10×10^3
Fluorine	F^-	1.3×10^6
Magnesium	Mg^{2+}	1.28×10^9
Arsenic	As(V)	1.2×10^3
Argon	Dissolved gas	0.62×10^6
Rubidium	Rb^+	0.12×10^6
Nickel		480
Zinc		350
Krypton	Dissolved gas	310
Caesium	Cs^+	306
Chromium	Cr(VI)	210
Antimony		200
Neon	Dissolved gas	160
Copper		150

lava is sufficient to boil it dry, providing the opportunity for the more reactive magnesium chloride salts, the last salts to form in the final stages of seawater evaporation [10], to hydrolyse on contact with dry steam and generate HCl gas [1]. Furthermore, [1] proposed that other salts (NaCl, KCl, $CaCl_2$) have a minimal role in the process. Laboratory studies and thermodynamic calculations indicate that the equilibrium sequence of salt precipitation from evaporating seawater at 25 °C is calcium carbonate when around 50–60% of the original volume of seawater remains, gypsum ($CaSO_4{\cdot}2H_2O$) and/or anhydrite ($CaSO_4$) when around 20% remains, halite (NaCl) when 9.5% remains, and K- and Mg-salts when <2% seawater remains [10]. Often, ancient evaporite sequences do not contain Mg- and K-salts owing to periodic recharge of seawater into the system, which prevented the evaporation process from proceeding to completion.

The variety of plausible magnesium chloride salts formed when seawater is boiled to dryness can be expressed as $MgCl_2{\cdot}nH_2O$, where the value of n can be 0, 1, 2, 4, or 6. Products resulting from the hydrolysis of

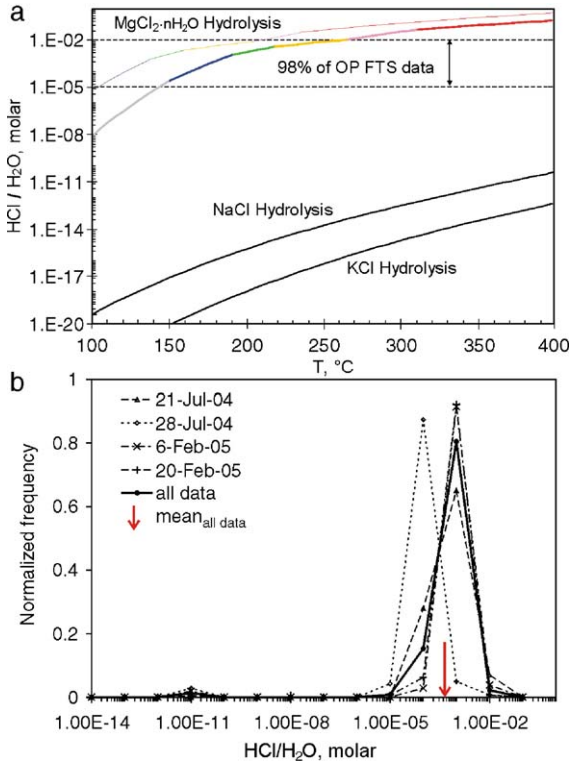

Fig. 5. (a) Model HCl/H_2O ratios for hydrolysis of magnesium chloride salts, NaCl and KCl compared to the range of 98% of the OP FTS HCl/H_2O values observed in this study. The thick-coloured curve represents hydrolysis of magnesium chloride salts based on reactions of types (3) and (4) at 0.1 MPa, as discussed in the text. Coloured line segments indicate the temperature stability ranges for reactant and product phases as follows: (grey) $MgCl_2{\cdot}6H_2O+Mg(OH)_2$ (100–150 °C); (blue) $MgCl_2{\cdot}4H_2O+Mg(OH)_2$ (150–191 °C); (green) $MgCl_2{\cdot}2H_2O+Mg(OH)_2$ (191–218 °C); (yellow) $MgCl_2{\cdot}H_2O+Mg(OH)_2$ (218–265 °C); (pink) $MgCl_2{\cdot}H_2O+MgO$ (265–310 °C); (red) $MgCl_2+MgO$ (>310 °C). The thin coloured line designates the following reactant-product temperature stability limits in a dry-steam interface film containing 90% air and CO_2: (blue) $MgCl_2{\cdot}4H_2O+Mg(OH)_2$ (<137 °C); (green) $MgCl_2{\cdot}2H_2O+Mg(OH)_2$ (137–159 °C); (yellow) $MgCl_2{\cdot}H_2O+Mg(OH)_2$ (159–203 °C); (pink) $MgCl_2{\cdot}H_2O+MgO$ (203–235 °C); (red) $MgCl_2+MgO$ (>235 °C). Note that the temperature stability ranges of the hydrated magnesium chlorides shift to lower values in the latter case because of the lower partial pressure of H_2O; the phase $MgCl_2{\cdot}6H_2O$ is no longer stable above 100 °C. There is a perceptible upward inflection in H_2O/HCl for both curves above the temperature at which MgO becomes stable (intersection of yellow and pink). (b) Histograms to show the range of measured molar HCl/H_2O on each of the four days and for all of the data. The mean HCl/H_2O (equal to 3.3×10^{-4}) and the range in which 80% of the data points lie (between 10^{-4} and 10^{-3}) are marked.

$MgCl_2 \cdot nH_2O$ include $Mg(OH)_2$ (brucite) and MgO (periclase) with release of HCl:

$$MgCl_2 \cdot nH_2O \rightarrow Mg(OH)_2 + (n-2)H_2O_{(gas)} + 2HCl_{(gas)} \quad (4)$$

$$MgCl_2 \cdot nH_2O \rightarrow MgO + (n-1)H_2O_{(gas)} + 2HCl_{(gas)}. \quad (5)$$

Thermodynamic equilibrium models based on reactions (4) and (5) allow calculation of HCl/H_2O ratios in dry steam films at the lava–seawater interface and are compared with values of HCl/H_2O measured in this study. Results are presented from 100 to 400 °C for dry steam interface films in shallow seawater (depths <10 m, total pressures <0.2 MPa), at 10 °C steps, after first determining the stable reactant and product solid phases over the 100–400 °C range (Fig. 5a). Thermodynamic data are from [11]. Equilibrium models may only be accurate for the lower end of this temperature range, but taking reaction kinetics into account for this particular case requires, in addition to the necessary rate equations, models of heat transfer rates for the lava–seawater system, which could be highly variable and complex. The equilibrium model offers a practical approach that can give approximate HCl/H_2O ratios at lower temperatures and useful insights into actual processes. The models assume unit activities for the solids and ideal gas behaviour. For these conditions and assumptions, HCl/H_2O is approximated by the square roots of the equilibrium constants for reactions of types (4) and (5). Fig. 5a shows the results at 0.1 MPa and includes, for comparison, the HCl/H_2O ratios calculated for the hydrolysis reactions of NaCl and KCl:

$$NaCl + H_2O_{(gas)} \rightarrow NaOH + HCl_{(gas)} \quad (6)$$

$$KCl + H_2O_{(gas)} \rightarrow KOH + HCl_{(gas)}. \quad (7)$$

The hydrolysis of calcium chloride ($CaCl_2$) yields HCl/H_2O ratios similar to those calculated for the alkali salts; however, calcium chlorides are generally not produced during seawater evaporation, since calcium is almost entirely consumed by early sulphate and carbonate formation ($CaSO_4$ and $CaCO_3$). Fig. 5b shows the HCl/H_2O molar ratios measured by OP FTS. The mean HCl/H_2O molar ratio for all of the data is 3.3×10^{-4}, 80% of the data lie in the range 10^{-4} and 10^{-3}, and 98% lie between 10^{-5} and 10^{-2}. It is clear from Fig. 5a that many orders of magnitude separate the molar HCl/H_2O resulting from hydrolysis of alkali chloride from the hydrolysis of magnesium chloride salts, and also that the range in HCl/H_2O measured in this study (Fig. 5b) is associated with the latter process.

The presence of silica as a reactant in NaCl hydrolysis (as suggested by [4]) increases the concentration of HCl in dry steam by an order of magnitude through formation of sodium silicate products [12], but this is not sufficient to account for the disparity in HCl/H_2O between the hydrolysis of alkali chloride salts and magnesium chlorides. The scatter in observed HCl/H_2O ratios (Fig. 5b) may be due to three effects. Scrubbing of HCl by water droplets with little simultaneous steam condensation [13] would tend to lower HCl/H_2O. The interface films may contain a significant fraction of air and CO_2 released from acidified brine (see below), which would elevate the HCl/H_2O curve (Fig. 5a) and would be especially pronounced for the hydrated magnesium chlorides at temperatures <~200 °C. An increase in pressure would decrease HCl/H_2O, but this effect is minor for the expected modest pressure increases (up to 0.3 MPa) that might occur near shallow ocean entries.

The HCl gas formed in the dry steam interface films dissolves into condensed water and boiled seawater brine droplets down-plume, forming acid aerosol particles within the airborne plume, which have been sampled by previous workers [3,4]. Our measurements of HCl gas near to the source of the plume show that this process occurs at plume ages of greater than at least a few seconds. For this to happen, it is essential that the HCl of the interface films is separated from the brucite and periclase products in order to prevent retrograde neutralization reactions. Investigations (by SEM/EDX, FTIR spectroscopy, X-ray powder photography, refractive-index measurements, and chemical staining tests) of samples of molten lava splashed with seawater showed that the solid products of these reactions ($Mg(OH)_2$ and MgO) formed coatings on the lava surfaces, together with abundant NaCl and other salts [14]. This suggests that similar deposits stick to the surfaces of ocean entry lava fragments which sink to the sea floor or are released as particles into a submarine lava–seawater interaction plume, an area of light-coloured seawater generally visible several miles westward down the coast.

It is of interest, as a historical note, that the hydrolysis of magnesium chlorides posed a severe problem in early determinations of the salinity of seawater by evaporation, drying, and weighing of salts, owing to the escape of HCl gas during the latter stages of evaporation, when a high temperature is required to remove the last traces of water [15]. The high reactivity of magnesium salts can be seen in experimental simulations of processes that could occur adjacent to radioactive waste canisters in underground repositories constructed in rock salt.

Studies were performed with electric heaters placed in holes drilled into the floor of the Waste Isolation Pilot Plant rock salt repository in the Salado Formation of the Delaware Basin, New Mexico, to simulate canister heating. Brine enriched in magnesium, potassium, sodium and chloride seeped into the holes [16] and deposits of magnesium chloride salts, $Mg(OH)_2$, and MgO formed on the high-temperature end of heaters where vaporisation was most intense, while hydrochloric acid condensate formed on heater components at lower temperatures, causing extensive corrosion [17].

4.2. Origin of CO_2 and NO_2 in the airborne lava–seawater interaction plume

Degassing of CO_2 from the magma occurs at localized areas at the summit and rift zones [18] and the lava is almost completely degassed of its CO_2 upon entry into the sea, making magmatic CO_2 an unlikely contributor to the lava–seawater interaction plume. Heavy, intense precipitation inland from the lava entry has frequently been observed [6], with the major-element composition of seawater [4]. This suggests that, in addition to condensed water from the evaporation of seawater, there are droplets of boiled seawater brine lofted into the atmosphere during small littoral explosions to become part of the plume. These droplets then provide a substrate for condensation of H_2O and HCl vapour co-generated by the lava–seawater interaction. Condensation acidifies the droplets of seawater brine, giving rise to highly acidic precipitation. A pH of 1.3 was measured in a condensate sample taken 9–11 m from the plume source [3], whilst a pH of 1.1–2.1 was measured in precipitation samples [4]. This acidity drives off the bicarbonate and carbonate contained in the brine as CO_2 gas through the reactions:

$$HCO_3^- + H^+ \rightarrow CO_{2(gas)} + H_2O_{(l)} \quad (8)$$

$$CO_3^{2-} + 2H^+ \rightarrow CO_{2(gas)} + H_2O_{(l)}. \quad (9)$$

Precipitation samples from ocean entries in 1991 and 1995 contained no remaining CO_3^{2-} or HCO_3^- above detection [4], which supports this interpretation. Seawater typically contains around 27 mg/kg inorganic carbon (Table 4), which would yield around 20 mg/kg CO_2 gas upon complete neutralization. Smaller amounts of CO_2 are probably produced from the acidification of local seawater near to the entry. A decrease in total dissolved CO_2 and alkalinity was measured in the seawater around the lava entry [4]; they suggested that this was due to the carbonate alkalinity of the seawater being titrated by the acidification. However, the acidification of boiled seawater brine droplets is likely to be much more intense than that of local seawater near entries, as the boiled seawater precipitation samples have a pH of 1–2 (and, consequently, zero CO_3^{2-}; [4]), whereas local seawater around the entries has a much higher pH of >6 and, consequently, an alkalinity of >1.5 meq/L and a $\sum CO_2$ of >1.8 mM [4].

The evaporation and boiling of seawater at entries could also cause CO_2 gas release related to calcium carbonate ($CaCO_3$) formation, which occurs after around 50% water loss, involving calcium and bicarbonate ions as reactants, yielding $CaCO_3$, CO_2 and H_2O as products [10]. The fallback of acidic particles onto the surface of the ocean will cause further minor acidification and CO_2 release downwind of the entries. Local heating of seawater will also lower the solubility of CO_2 (and other gases such as O_2) in the seawater, causing their exsolution. The processes discussed above, however, are likely to be much less important than the condensation of HCl on brine droplets entrained into the airborne plume in the generation of CO_2.

A possible source of gaseous NO_2 in the lava seawater plume is the thermal decomposition of nitrates in seawater. Coastal seawater contains inorganic nitrogen, in the form of nitrates and nitrites (NO_3^{2-} and NO_2^- ions; Table 4). These are produced from natural sources such as the oxidation of ammonium ions derived from the decomposition of organic material, fertilizers, sewage disposal systems and livestock facilities, which enter groundwater and eventually reach the sea. Concentrations of nitrate in the coastal waters of west Hawai'i have increased dramatically since the 1950s (up to 140 μmol/m^3 in west coast bays) and has been linked to eutrophication [19]. K_2NO_3 and Na_2NO_3 decompose on heating to KNO_2 and $NaNO_2$, respectively [20]. Thermal decomposition of $NaNO_2$ does not begin to take place until temperatures of around 600 °C are reached, generating Na_2O and NO_2 [20]. Nitrates of magnesium to copper in the reactivity series of metals (and ammonium nitrate) decompose on heating to ~400 °C, to form metal oxides, O_2 and NO_2 gas. Nitrate was detected in precipitation samples previously [3], which both confirms the presence of nitrates in the boiled seawater brine droplets and suggests that not all of the nitrate in the boiled seawater brine droplets is thermally decomposed during plume formation, possibly when some brine droplets are not boiled to dryness. Nitrates are found in ancient evaporite deposits, where they survived under conditions of gentle heating and evaporation (as opposed to the extreme temperatures at the lava–seawater entry) although their preservation is rare owing to their high solubility in water [19].

An alternative source of NO_2 is the fixing of nitrogen from the air and from nitrogen dissolved in seawater. HNO_3 was detected at mean concentrations of 5.6 μmol/m^3 at Lascar Volcano, Chile and 2.4 μmol/m^3 at Mount Etna, Italy [21]. It has been shown theoretically that heating air (or the gases dissolved in seawater) to temperatures up to 1400 K adjacent to basalt lava flows or at the top of a magma column could generate a significant mole fraction of NO in the air (approximately 6×10^{-4} for temperatures of around 1400 K) [21] through the thermal decomposition of N_2 [22]. NO was detected over the surfaces of active lava flows at Kīlauea at concentrations of up to 170 ppb [23]. NO oxidises to NO_2 (which probably accounts for 25% or less of the NO_2 produced from NO at low NO concentrations) or through photochemical reactions with radicals such as ozone and the peroxy radical. Oxidation rates of NO to NO_2 are low however, and it would take a few hours for a significant fraction of the thermal NO generated to be converted to NO_2 [24]. Further, the thermodynamical modelling presented earlier suggests that temperatures in the proximal lava–seawater interaction plume probably do not reach the temperatures required in order for significant thermal fixation of atmospheric N_2, as documented by [21], to occur.

The correlation between HCl and NO_2 (albeit weak; Fig. 3, Table 3) suggests the NO_2 is generated rapidly at the lava–seawater interface, consistent with the former process of rapid thermal decomposition of nitrates of magnesium, ammonium and calcium upon boiling seawater to dryness and then heating the dry nitrates to temperatures of around 400 °C. Larger amounts of NO_2 gas can be produced if the temperature of the steam plume reaches 600 °C, the temperature at which the thermal decomposition of potassium and sodium nitrite becomes significant. The NO_2 is removed from the plume downwind through conversion to nitric acid (HNO_3) by reaction with the hydroxyl radical and is removed rapidly from the plume by rain [24].

4.3. The origin of SO_2 in the lava–seawater interaction plume

SO_2 was detected on three days (Table 2, Figs. 2 and 3) but shows no consistent relationship with HCl in the plume, in contrast with the other species detected. We propose that the SO_2 is derived from the degassing of subaerial lava flows on the coastal plain. SO_2 exsolves from subaerial lava flowing from Pu‘u ‘Ō‘ō to the ocean, caused by delayed disequilibrium degassing and bubble rise through the flow during transport [25]. Small amounts of gases escape from the lava tubes through cracks in the tube roof and where lava breaks out. Downwind of the numerous degassing lava flows high SO_2 concentrations are possible which can easily be detected by OP FTS.

Sulphate enrichment (8% over that of seawater) in aerosol samples from the lava–seawater plume has been reported [4]. They ascribed the excess sulphate to degassing of the lava upon flowing into the sea, with SO_4^{2-} and F^- from the lava contributing 34±6% of the acidity in the precipitate samples, the rest from Na-metasomatism [4]. It appears unlikely that up to 40% of the acidity in the aerosol samples was generated from degassing of SO_2 and HF from lava. Lava degases efficiently and extensively during subaerial transport [25], so the melt is considerably depleted in volatile components by the time it reaches the sea and any release of volatiles upon reaching the sea will be minor, as this study shows. Instead, the acidity is proposed to be generated solely through the generation of HCl from the hydrolysis of $MgCl_2$ (discussed above). The sulphate enrichment in the condensate samples analysed by [4] can be explained by the presence of small fibres of gypsum and/or anhydrite. Boiling seawater increases the sulphate concentration until saturation of sulphate minerals is reached and they precipitate, beginning when around 20% of the original volume of seawater remains [10]. Sulphate was detected in silica-gel tube samples up to 1 mg/m^3 in concentration previously [3], but sulphuric acid was below detection. The presence of sulphate was ascribed to small fibres of calcium sulphate identified in the airborne samples by transmission electron microscopy analysis [3].

4.4. The mass flux of HCl from the lava–ocean entry

Thermal calculations are used to estimate the flux of HCl from the sea entry, based on the hydrolysis of magnesium chloride salts in seawater. The flux of lava from Pu‘u ‘Ō‘ō was estimated as 3.3 m^3/s for July 2004 and around 6.9 m^3/s for February 2005, based on the volume of magma necessary to account for the emission rate of SO_2 from Pu‘u ‘Ō‘ō [7]. It has been estimated that approximately one third of the extruded volume reaches the sea [26]. The mass of lava required to evaporate 1 kg of seawater is given by:

$$M_L = ((\Delta V_{SW} + E_{VAP})/(\Delta T \times C_{lava})). \quad (10)$$

where M_L is the mass of lava required to evaporate 1 kg seawater, ΔV_{SW} is the enthalpy change between seawater at 15 °C (63 kJ/kg) and 100 °C (419 kJ/kg),

E_{VAP} is the latent heat of vapourization of seawater (2261 kJ/kg at 100 °C), ΔT is the change in temperature of the lava (1100 to 100 °C) and C_{lava} is the heat capacity of basalt (0.84 kJ/kg/K). Around 2.8 kg of lava is required to evaporate 1 kg of seawater. The density of basalt is approximately 2800 kg/m^3; therefore, it will evaporate its own volume under ideal conditions. There are 0.1039 mol of chloride (associated with Mg salts) in 1 kg seawater. For a lava flux of 1 m^3/s, assuming that all of the lava cools to 100 °C rapidly enough to vaporise seawater and ideal thermal contact, the mass flux of HCl gas generated at the ocean entry is approximately 3.7 kg/s, or, if the entry is sustained, around 300 metric tonnes per day (t/d). In reality, only a small fraction of the lava will have thermal contact with the seawater at or near the ocean surface and the hydrolysis of magnesium chloride salts is expected to be incomplete, so this is a maximum. Cold lava fragments generated at the ocean entry are typically up to a few tens of centimetres across, which implies incomplete thermal contact with seawater. The HCl gas flux from small pāhoehoe lava ocean entries is therefore expected to be approximately 10–100 times smaller, yielding HCl mass fluxes in the range of 3–30 t/d. In February 2005 a correspondingly higher HCl flux from the sea entry (approximately double, due to higher lava effusion rates) was distributed between the three entries. The amount of HCl gas produced is not expected to be linear with the volume of lava reaching the sea owing to the lower surface area/volume ratio of large volume lava flows, which often maintain their coherence offshore. Optimum HCl production from seawater is likely to occur when the lava flows into the sea as ʻaʻā (which has a greater surface area/volume ratio than pāhoehoe flows) or when pāhoehoe flows subdivide. Once underwater, seawater is vaporised over the surface of the flows, but steam bubbles are quickly cooled and collapse a few centimetres away from the surface of the flow.

United States power plants and waste burning facilities produce about 2.5 Mt/yr HCl. Individual-emitting sources are regulated to producing no more than 1.8 kg/h, and stack gases must contain less than 50 ppm HCl. The largest source in the USA produces 8.2 t/d (Environmental Protection Agency), similar to a moderate-sized lava–sea entry. The mass flux of HCl from Puʻu ʻŌʻō crater and flank vents from magmatic degassing, was around 20–40 t/d [27]. The total flux of HCl from Kīlauea is therefore significantly increased during lava ocean entries if the lava–seawater interaction plume is also taken into account. Owing to the rapidity of HCl dissolution and rainout in the lava–seawater plume (and in the plume from Puʻu ʻŌʻō), this does not cause regional pollution, but it does produce high, localised concentrations of gaseous HCl and highly acidic precipitation.

During larger eruptions of Kīlauea and of Mauna Loa, the HCl flux from ocean entries might be significantly greater. In 1840, a Kīlauea eruption produced 215 million m^3 lava, of which 153 million m^3 reached the sea over 26 days [28]. This corresponds to a mean flux into the sea of around 68 m^3/s. The ocean entry was accompanied by *"loud detonations, fearful hissings and a thousand unearthly and indescribable sounds"* [28]. In 1919, a Mauna Loa eruption involved 152 million m^3 entering the sea in 10 days, a flux of around 176 m^3/s into the sea [29] and a 1950 eruption sent 76 million m^3 into the sea over 11 days [30], an average flux of 80 m^3/s. This ʻaʻā flow reached the sea at 1530 HST 2 June 1950, and a large, billowing cloud of steam arose. The flow maintained coherence and continued to flow several hundred metres offshore. By 1700 HST a line of steaming water extended from the shoreline along the course of the subaqueous flow. Close to shore and directly over the flow, the water was boiling, and an area of hot, turbulent water, where dead fish were floating, extended for 2 km [30]. The plume blew inland, causing heavy acid rain beneath it [30]. These ocean entries would have been associated with maximum HCl fluxes of 200–2200 t/d sustained over 2–4 weeks, which could have had a pronounced environmental impact on humans, vegetation and marine life.

Large emissions of gaseous HCl are also expected to accompany operations to divert lava flows using jets of seawater [31]. During the Eldfell eruption (Iceland) in 1973, 6.2 million metric tonnes of seawater were sprayed on advancing lava flows, cooling their surfaces and forming a thick crust, which prevented further flow and the destruction of Vestmannaeyjar [31]. The seawater formed thick steam clouds (there was very little run-off), produced at an average rate of around 0.4 m^3/s, which would have given rise to a similar, or slightly greater (owing to the involvement of ʻaʻā flows) mass flux of HCl gas to a typical lava ocean entry at Kīlauea, sustained over almost half a year, although the use of this method appears justified in the circumstances.

5. Conclusions

Open Path Fourier Transform infra-red Spectroscopy is a remote and accurate way in which to study the processes occurring in the gas phase of the airborne lava–seawater interaction plume at Kīlauea, Hawaiʻi. The gases H_2O, CO_2, HCl, NO_2 and SO_2 were detected

in the plume. Thermodynamic modelling of the hydrolysis reactions involving Mg salts compared with the hydrolysis of Na (and other) chloride salts show that the molar HCl/H_2O ratios measured in this study are in the range (10^{-4} to 10^{-3}) expected to accompany the hydrolysis of Mg salts to form HCl gas in the plume. The hydrolysis of Mg chloride salts at the lava–seawater interface is chiefly responsible for generating the HCl gas and the acidity of precipitates of the airborne plumes that develop near lava ocean entries. CO_2 is derived primarily from the breakdown of bicarbonate and carbonate ions in droplets of boiled seawater brine lofted into the plume as HCl and H_2O condense into them. NO_2 is probably derived from the thermal decomposition of dissolved nitrates in the seawater at around 400 °C. The temperatures required for significant fixation of atmospheric N_2 (>1100 °C) are probably not reached in this plume and the conversion from NO to NO_2 is too slow. Magmatic SO_2 degasses from subaerial lava flows on the coastal plain. The total mass flux of HCl from a typical ocean entry at Kīlauea lies in the range 3–30 t/d. The flux of HCl increases with the flux of lava flowing into the sea and is expected to be considerably higher during extensive ocean entries associated with large eruptions of Kīlauea or Mauna Loa and will cause substantial local and, possibly, regional effects such as acid rain.

Acknowledgements

This work was funded by the US Geological Survey's Mendenhall Postdoctoral Fellowship scheme. TMG thanks the late R.W. Decker for encouraging him to embark on this research and James Krumhansl and Kenneth Hon for sharing important insights and observations. Richard Herd provided invaluable assistance with fieldwork and manuscript editing. Jane Takahashi edited the manuscript prior to submission and improved it enormously. Tamsin Mather, John Stix and an anonymous reviewer are acknowledged for detailed and thorough reviews.

References

[1] T.M. Gerlach, J.L. Krumhansl, R.O. Fournier, J. Kjargaard, Acid rain from the heating and evaporation of seawater by molten lava: a new volcanic hazard, EOS (Trans. Am. Geophys. Un.) 70 (1989) 1421–1422.

[2] T.N. Mattox, M.T. Mangan, Littoral hydrovolcanic explosions; a case study of lava–seawater interaction at Kīlauea Volcano, J. Volcanol. Geotherm. Res. 75 (1997) 1–17.

[3] G.J. Kullman, W.G. Jones, R.J. Cornwell, J.E. Parker, Characterization of air contaminants formed by the interaction of lava and seawater, Environ. Health Perspect. 102 (1994) 478–482.

[4] J.A. Resing, F.J. Sansone, The chemistry of lava–seawater interactions: the generation of acidity, Geochim. Cosmochim. Acta. 63 (1999) 2183–2198.

[5] T.A. Jaggar, in: R.S. Fiske, T. Simkin, E.A. Nielsen (Eds.), The Volcano Letter, vol. 69, Smithsonian Institution, Washington, D. C., 1926

[6] J.G. Moore, R.L. Philips, R.W. Grigg, D.W. Peterson, D.A. Swanson, Flow of lava into the sea, 1969–1971, Kīlauea Volcano, Hawai'i, Geol. Soc. Am. Bull. 84 (1973) 537–546.

[7] A.J. Sutton, T. Elias, J. Kauahikaua, Lava effusion rates for the Pu'u 'Ō'ō-Kūpianaha eruption derived from SO_2 emissions and Very Low Frequency (VLF) measurements, USGS Prof. Pap., vol. 1676, 2003, pp. 137–148.

[8] G.A. Burr, R.L. Stephenson, M.M. Kawamoto, Health Hazard Evaluation report HETA 90-179-2172, National Institute for Occupational Safety and Health (NIOSH), 1990.

[9] Y. Nozaki, A fresh look at element distribution in the North Pacific, Eos, Transactions, American Geophysical Union, Electronic Supplement, May 1997.

[10] J.K. Warren, Evaporite Sedimentology: Importance in Hydrocarbon Accumulation, Prentice-Hall, Trenton, 1989, p. 285.

[11] A. Roine, Outokumpu HSC Chemistry for Windows — Chemical Reaction and Equilibrium Software with Extensive Thermochemical Database, Version 5.1, 02103-ORC-T, Outokumpu Research Oy, Pori Finland, 2002.

[12] R.O. Fournier, J.M. Thompson, Composition of steam in the system NaCl–KCl–H_2O–quartz at 600 °C, Geochim. Cosmochim. Acta 57 (1993) 4365–4375.

[13] A.H. Truesdell, J.R. Haizlip, H. Amannsson, F.D. Amore, Origin and transport of chloride in superheated geothermal steam, Geothermics 18 (1989) 295–304.

[14] T.M. Gerlach, unpublished data.

[15] J.P. Riley, R. Chester, Introduction to Marine Chemistry, Academic Press, London, 1971, p. 465.

[16] C.L. Stein, J.L. Krumhansl, A model for the evolution of brines in salt from the lower Salado Formation, southeastern New Mexico, Geochim. Cosmochim. Acta 52 (1988) 1037–1046.

[17] M.A. Molecke, N.R. Sorensen, J.L. Krumhansl, Summary of WIPP materials interface interactions: test data on metals interactions and leachate brine analyses, Sandia Report 88-2023C, Sand. Nat. Lab., Albuq., 1988, p. 19.

[18] T.M. Gerlach, E.J. Graeber, Volatile budget of Kīlauea Volcano, Nature 313 (1985) 273–277.

[19] D.J. Hoover, Fluvial nitrogen and phosphorus in Hawai'i: storm runoff, land use and impacts on coastal waters, PhD thesis (2002) University of Hawai'i.

[20] E.S. Freeman, The kinetics of the thermal decomposition of sodium nitrate and of the reaction between sodium nitrite and oxygen, J. Phys. Chem. 60 (1956) 1487–1493.

[21] T.A. Mather, A.G. Allen, B.M. Davison, D.M. Pyle, C. Oppenheimer, A.J.S. McGonigle, Nitric acid from volcanoes, Earth Planet. Sci. Lett. 218 (2004) 17–30.

[22] Y. Zeldovich, The oxidation of nitrogen in combustion and explosions, Acta Physicochim., USSR 21 (1947) 566–628.

[23] B. Huebert, P. Vitousek, A.J. Sutton, T. Elias, J. Heath, S. Coeppicus, S. Howell, B. Blomquist, Volcano fixes nitrogen into plant-available forms, Biogeochemistry 47 (1999) 111–118.

[24] J.A. Logan, Nitrogen oxides in the troposphere: Global and regional budgets, J. Geophys. Res. 88 (1983) 10785–10807.

[25] D.A. Swanson, B.P. Fabbi, Loss of volatiles during fountaining and flowage of basaltic lava at Kilauea Volcano, Hawai'i, J. Res. U.S. Geol. Surv. 1 (1973) 649–658.
[26] A.J.L. Harris, L.P. Flynn, S.K. Rowland, L. Keszthelyi, P.J. Mouginis-Mark, J.A. Resing, Calculation of lava effusion rates from Landsat-TM data, Bull. Volcanol. 60 (1988) 52–71.
[27] M. Edmonds, unpublished data.
[28] J.G. Moore, W.U. Ault, Historic littoral cones in Hawai'i, Pac. Sci. 14 (1965) 3–11.
[29] T.A. Jaggar, Monthly bulletin of the Hawaiian Volcano Observatory 7 (1919) 127–159, in: D. Bevens, T.T. Takahashi, T.L. Wright (Eds.), The Early Serial Publications of the Hawaiian Volcano Observatory, Hawaii Natural History Association, Hawaii National Park, vol. 2, 1988, pp. 1010–1044.
[30] G.A. MacDonald, Activity of Hawaiian Volcanoes during the years 1940–1950, Bull. Volcanol. 15 (1954) 120–179.
[31] R.S. Williams Jr., Lava-cooling operations during the 1973 eruption of Eldfell Volcano, Heimaey, Vestmanneayjar, Iceland, USGS Open File Rep., 1997, pp. 97–724.